

RESEARCH ARTICLE

Establishment and evaluation of a specific antibiotic-induced inflammatory bowel disease model in rats

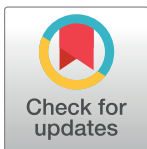
Guojun Tong^{1,2*}, Hai Qian¹, Dongli Li^{2‡}, Jing Li^{2‡}, Jing Chen^{2‡}, Xiongfeng Li³

1 Departments of General Surgery, Huzhou Central Hospital, Huzhou, Zhejiang, China, **2** Central Laboratory, Huzhou Central Hospital, Huzhou, Zhejiang, China, **3** Orthopedic Surgery, Huzhou Central Hospital, Huzhou, Zhejiang, China

☉ These authors contributed equally to this work.

‡ DL, JL, and JC also contributed equally to this work.

* tj97114@sina.com



OPEN ACCESS

Citation: Tong G, Qian H, Li D, Li J, Chen J, Li X (2022) Establishment and evaluation of a specific antibiotic-induced inflammatory bowel disease model in rats. PLoS ONE 17(2): e0264194. <https://doi.org/10.1371/journal.pone.0264194>

Editor: Pradeep Dudeja, University of Illinois at Chicago, UNITED STATES

Received: May 19, 2021

Accepted: February 6, 2022

Published: February 22, 2022

Copyright: © 2022 Tong et al. This is an open access article distributed under the terms of the [Creative Commons Attribution License](https://creativecommons.org/licenses/by/4.0/), which permits unrestricted use, distribution, and reproduction in any medium, provided the original author and source are credited.

Data Availability Statement: All relevant data are within the manuscript and its [Supporting Information](#) files.

Funding: YES. The present study was supported by Technology and Science Project of Zhejiang (grant no. 2018C37090). The funders had no role in study design, data collection and analysis, decision to publish, or preparation of the manuscript.

Competing interests: The authors have declared that no competing interests exist.

Abstract

Physical and chemical methods for generating rat models of enteritis have been established; however, antibiotic induction has rarely been used for this purpose. The present study aimed to establish and evaluate a rat model of inflammatory bowel disease (IBD) using antibiotics. A total of 84 Sprague-Dawley (SD) rats were divided into the following groups, according to the dosage and method of administration of the antibiotics: A, control; B, low-dose clindamycin; C, medium-dose clindamycin; D, high-dose clindamycin; E, low-dose clindamycin, ampicillin and streptomycin; F, medium-dose clindamycin, ampicillin and streptomycin; and G, high-dose clindamycin, ampicillin and streptomycin. Antibiotic administration was stopped on day 7; the modeling period covered days 1–7, and the recovery period covered days 8–15. Half of the animals were dissected on day 11, with the remaining animals dissected on day 15. Food and water intake, body weight and fecal weight were recorded. Intestinal flora was analyzed via microbial culture and quantitative PCR. The content of TNF- α , IL1- β , IL-6 and C-reactive protein (CRP) was assessed in abdominal aorta blood. Colonic and rectal tissues were examined pathologically via hematoxylin-eosin staining to assess leukocyte infiltration and intestinal mucosal changes as indicators of inflammation. Rat weight, food intake, water intake and 2-h fecal weight were significantly different across the experimental groups ($P = 0.040$, $P = 0.016$, $P < 0.001$ and $P = 0.009$, respectively). Microbial cultures revealed no significant differences between group A and B,C ($P = 0.546, 0.872$) but significant differences between group A and the other experimental groups (all $P < 0.001$). Furthermore, significant differences in the levels of *Bacteroides*, *Faecalibacterium prausnitzii* and *Dialister invisus* on day 4 between groups A, C and F ($P = 0.033$, $P = 0.025$ and $P = 0.034$, respectively). Significant differences were detected in the levels of TNF- α , IL1- β , IL-6 and CRP between the groups (all $P < 0.001$). The colonic and rectal pathological inflammation scores of the experimental groups were significantly different compared with group A (B vs. A, $P = 0.002$; others, all $P < 0.001$). These findings indicated that an antibiotic-induced IBD model was successfully established in SD rats; this animal model may serve as a useful model for clinical IBD research.

Introduction

Inflammatory bowel disease (IBD) includes Crohn's disease and ulcerative colitis (UC), which are common intestinal diseases that are increasing in incidence each year [1]. Clinically, patients with IBD exhibit a slow treatment effect and a long treatment period [2]. IBD is considered a disorder of the immune system [3]. Changes in the intestinal flora and its metabolites affect the patient's immune system, thereby inducing disease [4, 5]. IBD frequently involves activation of CD4+ T cells and dysregulation of TNF- α levels in circulating blood [6]; additionally, the disease commonly involves increased production of proinflammatory cytokines, such as IL-1 β and IL-6 [7]. Furthermore, C-reactive protein (CRP) has been observed to be upregulated in patients with IBD, rendering it a candidate biomarker for detecting IBD [8]. In order to obtain in-depth insight into the disease, animal models, such as rats, have been utilized [9–12]. Sprague-Dawley (SD) rats can be raised and controlled easily due to their mild temperament; hence, they have been used extensively for the establishment of various disease models [13]. Rat IBD models are primarily induced using chemical factors such as 2,4,6-trinitrobenzene sulfonic acid (TNBS) and [dextran sodium sulfate](#) (DSS) [11, 12, 14, 15]. These models are easy to induce with high reproducibility, and can simulate the acute and chronic inflammatory processes that occur in UC; however, they do not fully simulate UC lesions, and there are challenges associated with dosing when inducing these models [16]. Physical methods such as chemical enema or physical radiotherapy typically induce inflammation of the animal's rectum or sigmoid colon instead of total colorectal inflammation, and may cause mucosal and muscle acute necrosis; therefore, they do not accurately simulate UC or IBD observed in the clinic, limiting their utility [17]. Therefore, it is necessary to explore new methods of IBD modeling.

As imbalances in the intestinal flora may lead to enteritis, this has been used as a basis for modeling [18, 19]. Antibiotics frequently induce imbalances in the intestinal flora [20, 21]. Intestinal microbes are sensitive to clindamycin, ampicillin and streptomycin; thus, these antibiotics can easily cause intestinal microbial imbalance [22–27]. Therefore, the present study used different doses of clindamycin, as well as different combined doses of clindamycin, ampicillin and streptomycin, to disrupt the intestinal flora in rats. Inflammatory factors in the abdominal aorta, and the inflammation of the colon and rectum were analyzed to evaluate the utility of the model.

Materials and methods

Ethics

This study follows the Basel Declaration of 2010 and Institutional Animal Care and Use Committee (IACUC) of Xi'an United Nations Quality Detection Technology Co., Ltd. Laboratory (no reference number). All applicable international, national, and/or institutional guidelines for the care and use of animals were followed.

Rats

SD female rats ($n = 84$; age, 5–6 weeks; weight, 172.4–179.5 g) were obtained from Liaoning Changsheng Biotechnology Co., Ltd. All animals were quarantined and fed using a specific pathogen-free barrier system in the Xi'an United Nations Quality Detection Technology Co., Ltd. Laboratory for 9 days. All procedures were performed in accordance with the National Institute of Health Guide for the Care and Use of Laboratory Animals [28]. All experimental procedures and animal handling were performed in accordance with the guidelines of the International Association for the Study of Pain, and the animal protocols were approved by

the Xi'an United Nations Quality Detection Technology Co., Ltd. Animal Committee. The authors made an effort to minimize the number of animals used.

Experimental drugs, reagents and instruments

The drugs used in the present study were as follows: Clindamycin hydrochloride (cat. no. C10038638; Shanghai Macklin Biochemical Co., Ltd.), 99% purity; ampicillin (cat. no. L220S26; Hebei Bailingwei Superfine Material Co., Ltd.), 98% purity; and streptomycin (cat. no. 20171123; Tianjin Guangfu Fine Chemical Research Institute), $\geq 90\%$ purity.

Rat IL-1 β (rat.no.20884), IL-6 (YPH102698), TNF- α (EK0526) and C-reactive protein (CRP) ((cat. no. 201810).ELISA kits were obtained from Bioswamp Life Science LabA soil genomic DNA rapid extraction kit, rapid competent cell preparation kit (one-step method), SanPrep column plasmid DNA small amount extraction kit (cat. no. B518191-0050) and San-Prep column DNA gel recovery kit (cat. no. B518131-0050) were all purchased from Sangon Biotech Co., Ltd. Taq Plus DNA polymerase (cat. no. B600090), agarose B (cat. no. A600014) and 4S Red Plus Nucleic Acid Stain (10,000X aqueous solution; cat. no. A606695) were from BBI (Sangon Biotech Co., Ltd.). GeneRuler DNA Ladder Mix was procured from Thermo Fisher Scientific, Inc. A pMD[™]18-T Vector Cloning kit was obtained from Takara Biotechnology, Co., Ltd.

Bacteroides-Bile-Enterprise (BBE) agar (cat. no. 20171215; Qingdao Hope Bio-Technology Co., Ltd.), *Lactobacillus* selective agar (cat. no. 20180424; Qingdao Hope Bio-Technology Co., Ltd.), anaerobic bacteria agar (cat. no. 171209; Beijing Luqiao Technology Co., Ltd.), trypticase-phytone-yeast (TPY) agar medium (cat. no. 180208; Beijing Luqiao Technology Co., Ltd.), mannitol sodium chloride agar medium (cat. no. 171008; Beijing Luqiao Technology Co., Ltd.), eosin methylene blue (EMB) agar (cat. no. 160504; Beijing Luqiao Technology Co., Ltd.), CATC agar (cat. no. 20170902; Qingdao Hope Bio-Technology Co., Ltd.), and reinforced *Clostridium* culture medium (cat. no. 171117; Beijing Luqiao Technology Co., Ltd.) were purchased for bacterial culture.

An Electric Day constant temperature incubator was purchased from Tianjin Taisite Instrument Co., Ltd. (cat. no. DH6000BII). A LabSystems Multiskan MS 352 microplate reader was purchased from Thermo Fisher Scientific, Inc. A low-speed condensation centrifuge was purchased from Shanghai Lu Xiangyi Centrifuge Instrument Co., Ltd (cat. no. DDL-5M). An upright microscope was purchased from Nikon Corporation.

The following instruments were utilized for quantitative (q)PCR: High-speed refrigerated centrifuge (cat. no. HC-2518R; Anhui Zhongke Zhongjia Science Instrument Co., Ltd.); electrophoresis instrument (cat. no. DYY-6C; Beijing Liuyi Biotechnology Co., Ltd.); electrophoresis tank (cat. no. H6-1; Shanghai Jingyi Plexiglass Products Instrument Factory); gel imaging system (cat. no. FR980; Shanghai Furi Science & Technology Co., Ltd.); micro spectrophotometer (cat. no. SMA4000; Merinton Instrument, Inc.); PCR machine (Bio-Rad Laboratories, Inc.); and a generation sequencer and StepOne[™] fluorescence quantitative PCR instrument (Applied Biosystems; Thermo Fisher Scientific, Inc.).

Animal grouping and modeling

The animals were grouped as follows: A, control group, normal saline; B, low-dose clindamycin group (250 mg/kg); C, medium-dose clindamycin group (500 mg/kg); D, high-dose clindamycin group (750 mg/kg); E, low-dose triple antibiotic group (clindamycin, ampicillin and streptomycin; 250, 272.1 and 136.1 mg/kg, respectively); F, medium-dose triple antibiotic group (clindamycin, ampicillin and streptomycin; 500, 563.7 and 281.8 mg/kg, respectively); and G, high-dose triple antibiotic group (clindamycin, ampicillin and streptomycin; 750, 835.8

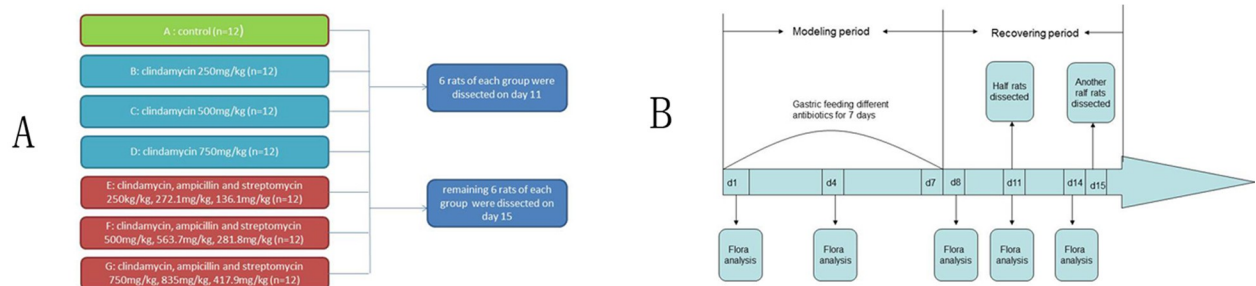


Fig 1. Study flow and method. (A) Group design of the study. (B) Experimental work flow of the study.

<https://doi.org/10.1371/journal.pone.0264194.g001>

and 417.9 mg/kg, respectively). The experiment was divided into two stages: The modeling period (days 1–7) and the recovery period (days 8–15). The administration volume was 10 ml/kg/day intragastrically using an oral needle during the modeling period between 8:30–10:00 a.m. The intragastric administration was stopped on day 8. Animal weight, and food and water intake were monitored, and stool samples were collected on days 1, 3, 5, 7, 9, 11 and 14 within 2 h post-administration of antibiotics. For each rat, the fecal microbial flora was examined on days 1, 4, 8, 11 and 14. On days 11 and 15, under sodium pentobarbital anesthesia (intraperitoneal; 2%; 40 mg/kg), the abdominal walls of 50% of the animals in each group were cut, the abdominal aorta exposed and abdominal aortic blood drawn (Fig 1A and 1B). Then, the rats were dissected after being euthanized via exsanguination whilst under anesthesia by cutting the abdominal aorta, and death was confirmed by the pulsation of the abdominal aorta disappearing and the pupils dilating, after which colonic and rectal tissues were collected.

Microbial culture

The microbial species detected were *Staphylococcus aureus*, *Bifidobacterium*, yeast, *Bacteroides*, *Clostridium*, anaerobic bacteria, *Escherichia coli* (*E. coli*), *Enterococcus* and *Lactobacillus*. An equivalent of 1 g feces was mixed with 9 ml tryptone soy broth. A volume of 20 μ l of the appropriately diluted sample was spread evenly on mannitol sodium chloride, EMB and CATC agar plates and cultured under aerobic conditions at 37°C for 48 h. The above organisms were also cultured on TPY, BBE, reinforced *Clostridium* medium, anaerobic and *Lactobacillus* selective agar plates at 37°C for 48 h in anaerobic conditions. Organisms inoculated on dichloran rose-Bengal chloramphenicol agar plates were cultured for 5 days at 28°C in aerobic conditions. The colonies were stained by methylene blue and enumerated using the following formula: Number of colonies (CFU/g) = number of plate colonies \times 50 \times dilution factor, with $\times 10^6$ used as the uniform independent unit.

Diarrhea within 2 h after administration

Within 2 h after drug administration on days 1, 4, 8, 11 and 14, the number of defecations of each rat in each group was counted to determine whether they exhibited diarrhea, as well as the severity of diarrhea if present. If >2 defecations were observed, then diarrhea was considered to be present. Additionally, changes in the diet and water consumption of rats were monitored. It was observed that the rats exhibited no obvious signs of dehydration and could tolerate the experimental protocol.

qPCR analysis

A soil genomic DNA rapid extraction kit was used to extract fecal DNA from SD rats as follows: i) SD rat feces (400 mg) was mixed with 400 μ l of 65°C pre-warmed Buffer SCL via

agitation in a 65°C water bath for 5 min; ii) supernatant (350 µl) was obtained via centrifugation at 2,250 x g for 3 min at room temperature; iii) an equal volume of Buffer SP was mixed via inversion, and placed on an ice bath for 10 min; iv) centrifugation was conducted at 2,250 x g for 3 min at room temperature; v) the resulting supernatant was mixed with chloroform, followed by centrifugation at 2,250 x g for 3 min at room temperature; vi) the upper aqueous phase was mixed with 2 volumes of absolute ethanol via inversion and incubated at room temperature for 3 min, followed by centrifugation at 1570g(rcf) for 5 min at room temperature; vii) ethanol (75%; 1 ml) was added to the pellet for washing via centrifugation at 2,250 x g for 3 min at room temperature, with this step repeated; viii) the residual ethanol is allowed to evaporate; and ix) the resulting DNA pellet is solubilized in 70 µl TE Buffer. qPCR was performed using a pMD18-T Vector Cloning kit, Taq polymerase and a StepOne fluorescence quantitative PCR instrument. Of the aforementioned nine microbiota, only *Bacteroides* was successfully detected via PCR. Therefore, fecal matter was collected on day 4, and the presence of *Bacteroides*, *Faecalibacterium prausnitzii* (*F. prausnitzii*) and *Dialister invisus* (*D. invisus*) was analyzed via qPCR. Gene fragments from *Bacteroides*, *F. prausnitzii* and *D. invisus* were retrieved from the NCBI GenBank database (<https://www.ncbi.nlm.nih.gov/genbank/>); the primers used are presented in S1 Table. The amplicons were analyzed via 1.5% agarose gel electrophoresis and ethidium bromide was excited by standard 302nm ultraviolet transmittance. Bands were imaged using a DNA gel electrophoresis imager (Analytik Jena AG) and quantified using Quantity One v4.6.6 (Bio-Rad Laboratories, Inc.).

Analysis of inflammatory factors

On days 11 and 15, half of the rats in each group were dissected under intraperitoneal anesthesia as aforementioned. The abdomen was cut, and 5 ml blood was withdrawn from the abdominal aorta. Blood serum (0.5 ml) was obtained from each sample via centrifugation at 1,570 x g for 3 min at 4°C. The content of TNF- α (EK0526), IL-1 β (rat.no.20884), IL-6 (YPH102698), and CRP (cat.no.2018) was detected in the blood serum without diluting via ELISA according to the manufacturer's protocols.

Colonic and rectal pathological inflammation assessment

We choose the relative same part of colon and rectum for pathological analysis on days 11 and 15. All tissues were stained using hematoxylin-eosin before inflammation assessment. The hematoxylin-eosin staining process were as follows: Tissues were fixed in 10% formaldehyde at room temperature for 10 min, embedded in paraffin and cut into sections (5–8 µm). The sections were stained in hematoxylin for 5 min and alcohol eosin staining solution for 2–3 min at room temperature. An upright light microscope was used to analyze the stained tissues (magnification, x200). The degree of neutrophil infiltration and intestinal mucosal changes were graded as follows: 0, no inflammation; 1, low multifocal neutrophil infiltration [<10 neutrophils/high-powered field (HPF)]; 2, moderate multifocal neutrophil infiltration (submucosal involvement; 10-50/HPF); 3, extensive multifocal and aggregated neutrophil infiltration (submucosal involvement and muscle layer; >50 /HPF); 4, additional abscesses or extensive muscle layer involvement [15, 29]. Each section was analyzed in three fields, and the score in each section was added to produce the final score.

Statistical analysis

Primer Premier 5.0 software (Premier Biosoft International) was used for designing the primers. The data were analyzed using SPSS 21 software (IBM, Corp.). Continuous data were analyzed using one-way ANOVA followed by Tukey post hoc test, and are presented as the mean

\pm SD. Ordinal data were analyzed using Kruskal-Wallis H test and Dunn's post hoc test, and are presented as the median and interquartile range. $P < 0.05$ was considered to indicate a statistically significant difference.

Results and discussion

Comparison of basic indices

The present study aimed to establish an antibiotic-induced rat IBD model. Previous studies have conducted comparative research on rat IBD models induced using different chemical factors, and speculated the various advantages and disadvantages of models induced using agents such as TNBS and DSS [11, 12, 14]. IBD is a group of chronic inflammatory disorders that affect individuals throughout life. Although factors involved in the etiology and pathogenesis of IBD remain unknown, studies using animal models of colitis have indicated that dysregulation of host/microbial interactions is a requisite for the development of IBD [30–32]. As we know, IBD usually causes changes in diet, weight and stool. The average starting weight of all rats was 172.6 ± 2.49 g, and no significant difference was detected in the weight between groups A-G before experiment ($P > 0.05$). Significant differences between groups were observed for the mean weight, food intake, water intake and stool in 2 h post-administration on days 1, 3, 5, 7, 9, 11, 13, 14 between groups and some significant difference were observed within groups (S2 Table and Fig 2). The mean weight, food intake, water intake and stool in 2h increases significantly not dependent on dosage and method of administration. These results may come from comprehensive calculation of different days.

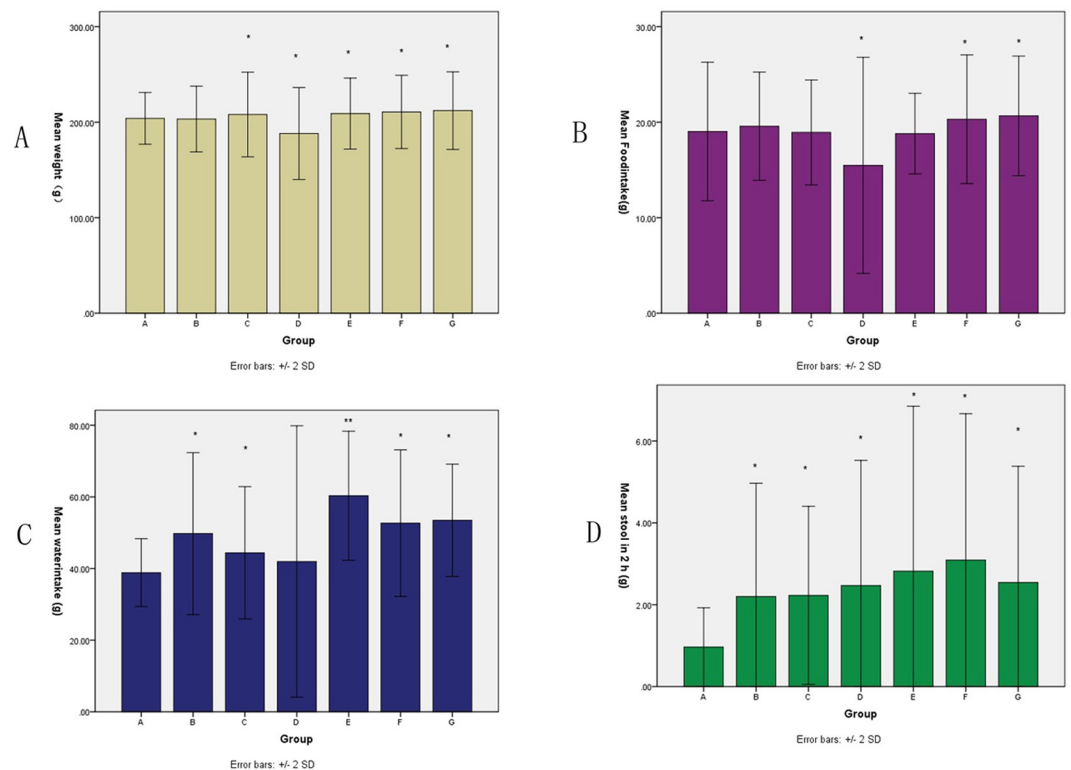


Fig 2. Mean basic characteristics on days 1,3,5,7,9,11,13,14. (A) Comparison of animal weights (B) Comparison of food intake of the animals (C) Comparison of water intake of animals (D) Comparison of stool within 2 h. Data are presented as the mean \pm SD. Treatment groups vs control groups: * < 0.05 ; ** < 0.001 .

<https://doi.org/10.1371/journal.pone.0264194.g002>

Comparison of nine microbes between groups

S. aureus, *Bifidobacterium*, yeast, *Bacteroides*, *Clostridium*, anaerobic bacteria, *E. coli*, *Enterococcus* and *Lactobacillus* were cultured using special medium, and the number of colonies was counted [Fig 3]. Levels of beneficial bacteria (*Bifidobacterium*, *Clostridium*, *Lactobacillus*) decreased significantly, while pathogenic bacteria (*S. aureus*, yeast, *Bacteroides*, anaerobic bacteria, *E. coli*, *Enterococcus*) levels increased significantly (Fig 4). The total microbial load of the nine species was calculated and compared between the control and experimental groups (S3 Table). Microbial cultures revealed no significant differences between group A and B,C ($P = 0.546, 0.872$) but significant differences between group A and the other experimental groups (all $P < 0.001$). The mean levels of the nine microbes in each group were significantly different on days 1, 4, 8, 11 and 14 respectively (all $P < 0.001$; Fig 5A–5E). A previous study utilized a similar method to study gut microbiota, finding that 4-week administration of an antibiotic cocktail depressed the ventilator response to hypercapnic stress in conscious animals [33]. This study also found that microbiota-depleted rats exhibited decreased systolic blood pressure, and that chronic antibiotic intervention or fecal microbiota transfer resulted in disruptions to brainstem monoamine neurochemistry that were associated with the abundance of various bacteria. In the present study, changes in the 9 microbiota in different days were observed. *S. aureus* is a major human pathogen that causes a wide range of clinical infections [34, 35]. *Bifidobacterium* is a group of living microorganisms commonly included in supplements that confer health benefits on the host when administered in sufficient quantities [36]. *Bifidobacterium* levels were significantly reduced in the experimental groups compared with the

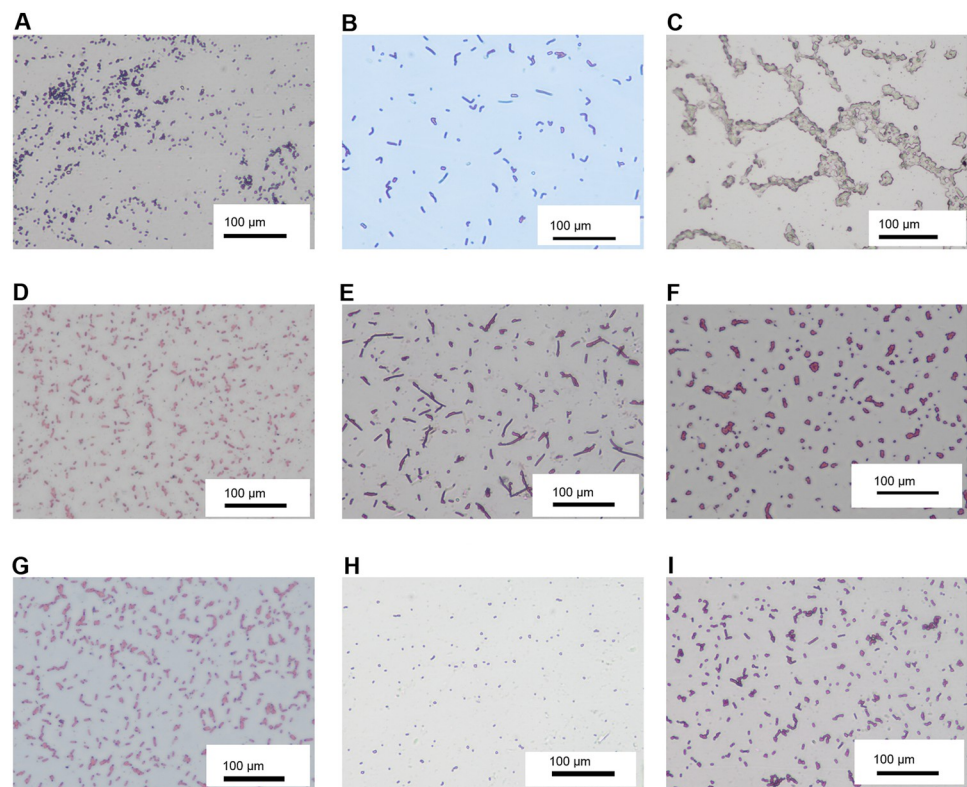


Fig 3. Microbial specimens from rat feces under a microscope on day 4 (methylene blue staining, x100). (A) *Staphylococcus aureus*, (B) *Bifidobacterium*, (C) yeast, (D) *Bacteroides*, (E) *Clostridium*, (F) anaerobic bacteria, (G) *Escherichia coli*, (H) *Enterococcus* and (I) *Lactobacillus*.

<https://doi.org/10.1371/journal.pone.0264194.g003>

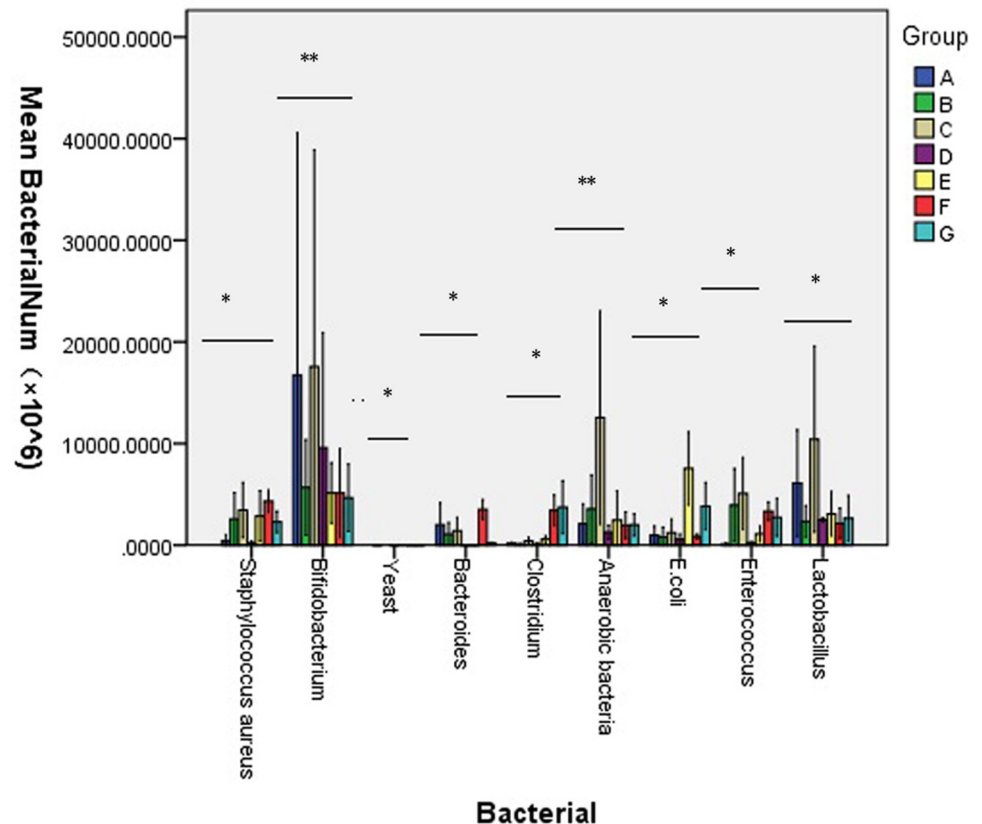


Fig 4. Comparison of nine types of microflora in the feces between A to G groups. The results show the levels of beneficial bacteria (*Bifidobacterium*, *Clostridium*, *Lactobacillus*) decreased significantly, while pathogenic bacteria (*S. aureus*, yeast, *Bacteroides*, anaerobic bacteria, *E. coli*, *Enterococcus*) levels increased significantly.* $P < 0.05$, ** $P < 0.001$.

<https://doi.org/10.1371/journal.pone.0264194.g004>

control group.(Fig 4) *Yeast* is often employed in industrial fermentation processes due to its ability to efficiently convert relatively high concentrations of sugars into ethanol and carbon dioxide [37]. *Yeast* is not a common intestinal bacterium and was absent in the control group; it was only detected in the low- and medium-dose triple antibiotic groups. *Bacteroides* is a gram-negative, non-spore, obligate anaerobic bacillus [38, 39]. *Clostridium* species are anaerobic, gram-positive, rod-shaped, endospore-forming bacteria belonging to the phylum *Firmicutes*, and they constitute both a class and a genus within the phylum [40]. *Clostridium* levels decreased in the single-agent groups, but increased in the combined drug group.(Fig 4) Anaerobic bacteria serve pivotal roles in the microbiota of humans; these are also infectious agents involved in various pathological processes such as *ChuW*, *ChuX* and *ChuY* which were contiguous genes downstream from a single promoter that were expressed in the enteric pathogen.[41]. Pathogenic variants of *E. coli* cause substantial morbidity and mortality worldwide [42]. *Enterococcus* strains adhere strongly to the intestinal epithelium, forming biofilms, and possess antioxidant defense mechanisms that affect inflammatory processes [43]. The genus *Lactobacillus* consists of 173 species, evolutionary relationships between lactobacilli can be analyzed using core-genome trees [44]. Due to their symbiotic roles in humans, when lactobacilli mutate, they can produce infectious diseases such as colpitis and pelvic infection [45]. Antibiotic-induced gut dysbiosis induces various effects on the body. Liu *et al* [46] and Yu *et al* [47] considered the effects on body metabolism. Other studies reported associated effects on the nervous system [48–50]. Additional studies identified effects on tumor progression [51, 52]. Additional effects in other physiological systems, such as the immune

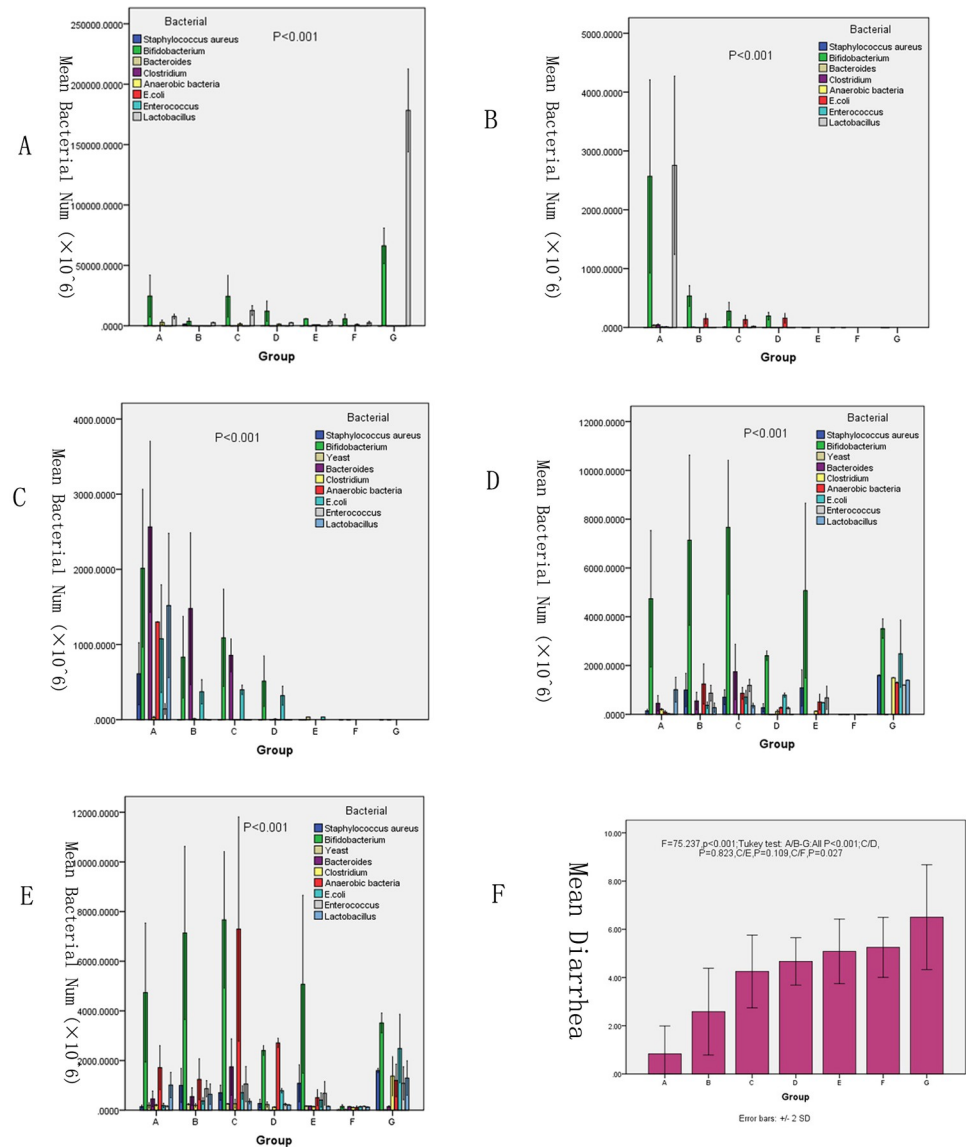


Fig 5. Nine types of microflora in the feces of experimental rats. (A) Comparison on day 1, (B) Comparison on day 4, (C) Comparison on day 8, (D) Comparison on day 11 and (E) Comparison on day 14. (F) Defecation of rats within 2 h of antibiotic administration across the study period. Data are presented as the mean \pm SD.

<https://doi.org/10.1371/journal.pone.0264194.g005>

system [53] and intestinal barrier [54, 55], have been reported. Due to these various possible effects, antibiotic-induced gut dysbiosis requires further investigation. In the present study, with increasing dose of antibiotics and enhanced effect when antibiotics were combined, levels of beneficial bacteria (*Bifidobacterium*, *Clostridium*, *Lactobacillus*) decreased significantly, while pathogenic bacteria (*S. aureus*, yeast, *Bacteroides*, anaerobic bacteria, *E. coli*, *Enterococcus*) levels increased significantly.

Diarrhea analysis

The number of defecations within 2 h after drug administration were counted for each rat in each group across all included days (days 1, 4, 8, 11 and 14; S4 Table). Mean defecations in

groups A-G across all included days were 0.833 ± 0.578 , 2.583 ± 0.900 , 4.250 ± 0.754 , 4.667 ± 0.492 , 5.083 ± 0.669 , 5.250 ± 0.622 and 6.500 ± 1.087 , respectively. Using one-way ANOVA and Tukey post hoc test, it was observed that all experimental groups exhibited significantly greater defecation than group A (all $P < 0.001$; Fig 5F). IBD often results in diarrhea [56]. The present study showed that all doses and antibiotic treatments induced significant diarrhea compared with the control group. Patients with IBD often sufferer from diarrhea; the present study observed that diarrhea was exacerbated with increased dose. It is proposed that the extent of diarrhea was related the degree of intestinal microbiota disorder and intestinal inflammation.

qPCR analysis of three strains

The concentrations of DNAMarks, *Bacteroides*, *F. prausnitzii* and *D. invisus* in A,C,F groups on fourth day were compared via qPCR. The same DNA marks expressed differently in the three gene fragments. One-way ANOVA revealed significant effects of treatment on the levels of DNA mark ($P = 0.044$), *Bacteroides* ($P = 0.036$), *F. prausnitzii* ($P = 0.027$) and *D. invisus* ($P = 0.036$). Post hoc analysis revealed significant decreases in quantity of *Bacteroides*, *F. prausnitzii* and *D. invisus* between group F and group A (all $P < 0.01$), as well as between group F and group C ($P < 0.01$ for *Bacteroides*, otherwise $P < 0.05$; Fig 6A and 6B, S1 Raw Image). *Bacteroides*, *F. prausnitzii* and *D. invisus* are associated with IBD [57–59]. Thus, qPCR analysis of these three strains was performed in groups A, C and F, after attempts to perform qPCR analysis of the aforementioned nine types of microbiota were unsuccessful. The results showed that decreased quantities of these bacteria were observed following combination antibiotic

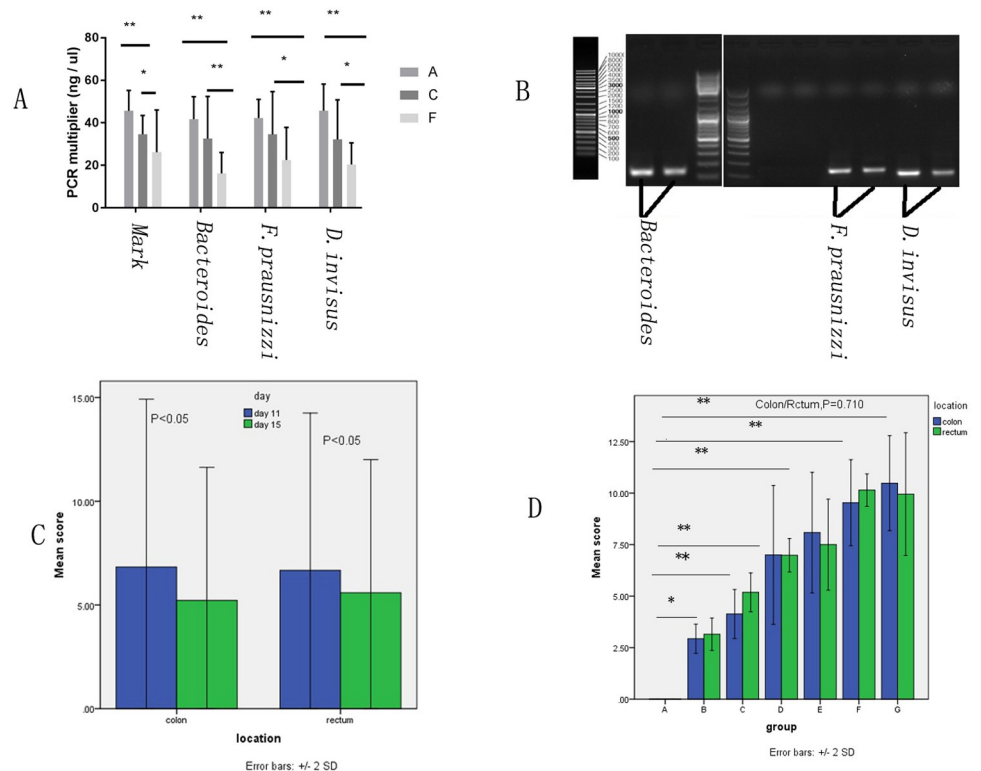


Fig 6. Fecal bacterial content and gut inflammation scores. (A) Comparison of bacterial amplification via quantitative PCR in groups A, C and F; (B) *Bacteroides*, *F. prausnitzii* and *D. invisus* agarose electrophoresis; (C) Comparison of colonic and rectal tissue inflammation scores on day 11 and day 15; (D) Comparison of colonic and rectal tissue inflammation scores of control group vs experiment groups respectively, * $P < 0.05$, ** $P < 0.01$.

<https://doi.org/10.1371/journal.pone.0264194.g006>

treatment compared with clindamycin alone. *Bacteroides* species constitute a large part of the human gut microbiota, including both probiotics and pathogenic bacteria (depending on various genetic and environmental factors), and can cause disease conditions as varied as skin infections, endocarditis, intra-abdominal sepsis, appendicitis, bacteremia, pericarditis, meningitis and brain abscesses [60–62]. There is currently increasing interest in *F. prausnitzii*, one of the most abundant enteric microorganisms. However, whether there are other strains within this species and whether there are other *Faecalibacterium* species remain unclear [63, 64]. *D. invisus* levels are low or absent in patients with IBD [65]. The present study showed that *D. invisus* was only observed in small quantities in rat feces, with smaller levels in model groups.

Changes in abdominal aortic inflammatory factors

The levels of TNF- α , IL1- β , IL-6 and CRP in serum from the abdominal aorta were evaluated, and one-way ANOVA revealed significant effects of group type on the levels of these factors (All $P < 0.001$; S4 Table, Fig 7). Post hoc analysis revealed significant increases in the levels of all these factors in the experimental groups compared with group A ($P = 0.001$, group B vs. group A for IL-1 β ; others, all $P < 0.001$). The present study found that abdominal aortic blood levels of TNF- α , IL-1 β and IL-6 were significantly upregulated in all groups compared with the control group. TNF- α has been reported to be a potent stimulator of IL-6 production [66–68].

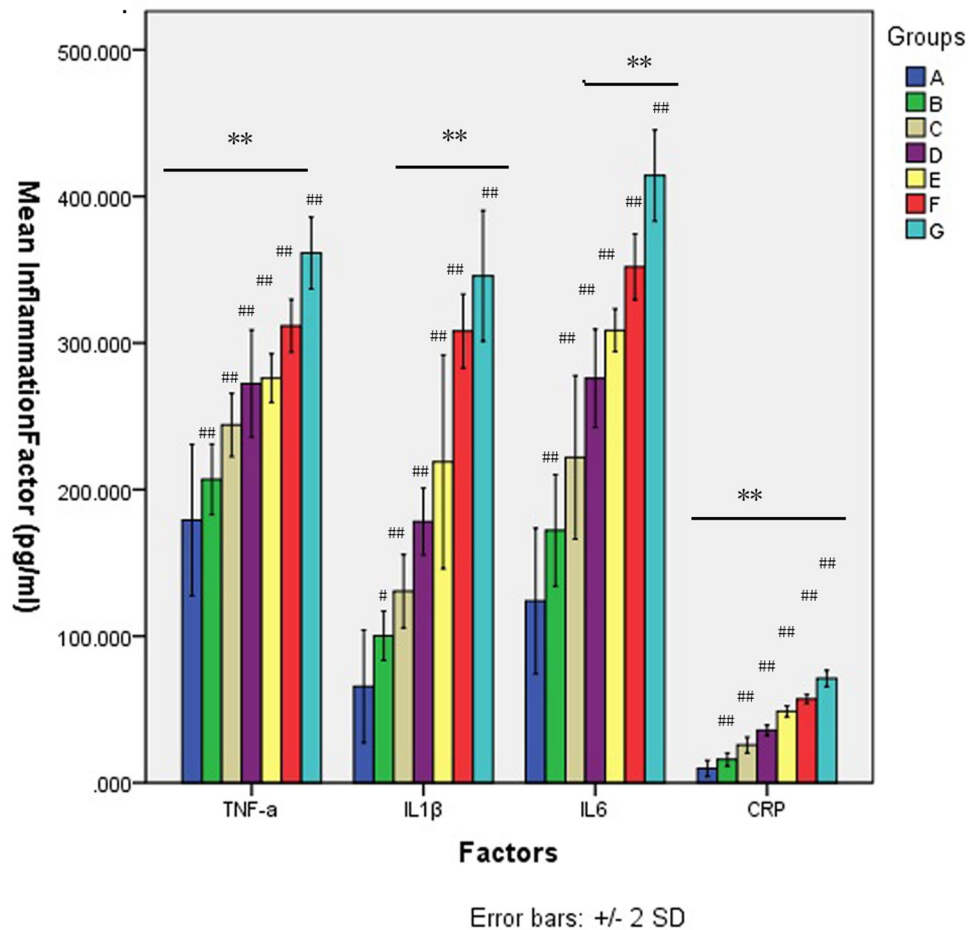


Fig 7. Comparison of inflammation factors between groups and within groups. ** $P < 0.001$, Comparison between groups; # = 0.001, ## < 0.001 , Comparison for experiment groups vs control groups.

<https://doi.org/10.1371/journal.pone.0264194.g007>

Inflammation induces IL-1 β production in Kupffer cells and hepatocytes [69]. CRP is increasingly studied within the context of inflammation and associated diseases [70–72]. The present study found that elevated CRP was detected in groups that received antibiotics compared with the control group.

Comparison of pathological inflammation scores

Colonic and rectal tissues were scored for pathological inflammation after hematoxylin-eosin staining. These data were analyzed using Kruskal-Wallis H test followed by Dunn's post hoc test. Significant differences in inflammation were observed between group A and all experimental groups ($P = 0.002$ for group B vs. group A, all other comparisons vs. group A, $P < 0.001$; [S5 Table](#)). We found that pathologic inflammation scores increased with the increasing of dosage and combined administration. ([Fig 6C and 6D](#)) However, no significant difference was detected in the degree of inflammation between the two tissues ($P = 0.710$; [Fig 6D](#)). Additionally, inflammation scores were significantly higher on day 11 compared with day 15 within groups for both colonic and rectal tissues ([Fig 6C](#)). Pathologic colonic and rectal sections for control group and different experimental groups are presented in [Figs 8 and 9](#). Pathological examination is important for evaluating the degree of tissue inflammation. Colonic and rectal tissues were scored based on the degree of neutrophil invasion. It was observed that the degree of inflammation in the intestinal mucosa of rats dissected on day 11 was more severe than in rats dissected on day 15, which may be related to self-recovery of the intestinal flora. The dysregulation of host-microbiota interactions in the gut is a pivotal characteristic of Crohn's disease [73]. However, whether commensals and/or the dysbiotic microbiota associated with pathology in humans are causally involved in Crohn's pathogenesis remains controversial [73]. In the present study, the degree of inflammation of the colon and rectal tissues was investigated in antibiotic-induced SD rat enteritis models. It was found that with increasing dose or number of antibiotics used, the more severe the inflammation of the colonic and rectal tissues. ([Fig 6D](#)) This phenomenon may be associated with the release of inflammatory factors by the disordered intestinal flora [74], or with damage of intestinal mucosa caused by the release of metabolites by pathogenic microbiota, which induces humoral and cellular immunity [74, 75]. Improper use of antibiotics induces intestinal flora imbalance, which can cause changes in metabolism [46, 47] and the production of novel metabolites, such as hydrogen sulfide [76]. This altered metabolism induces changes in body fluids and cellular immunity [53], thereby destroying the intestinal mucosa of the body, leading to intestinal inflammation and the formation of intestinal ulcers, which may induce IBD [53]. The present study demonstrated gut inflammation induced by antibiotics in the proposed IBD model. In addition, the improper use of broad-spectrum antibiotics can also lead to obesity [77].

The present study has some limitations, such as a lack of information concerning the inflammatory factors with respect to intestinal mucosa necrosis, as well as the mechanisms connecting IBD and immune function within the body. In this paper, we did not explore whether enteritis caused by intestinal microbial disorder was caused by cellular immune attack or humoral immune attack. At the same time, we had not studied the signaling pathway of this mechanism. For example, we did not analyze the changes of CD4+ and CD8+ in tissues of different groups and we did not elaborate whether the mechanism of intestinal inflammation was similar to that of DSS and TNBS mice, eg. whether T helper cells played a role in information transmission. These may lead us to the direction of further research in the future. Additionally, flow cytometric analysis was not performed to examine immune cell populations in the different groups. Meanwhile, we did not compare and correlate the inflammatory markers in the histology with the altered cytokine mRNA expression.

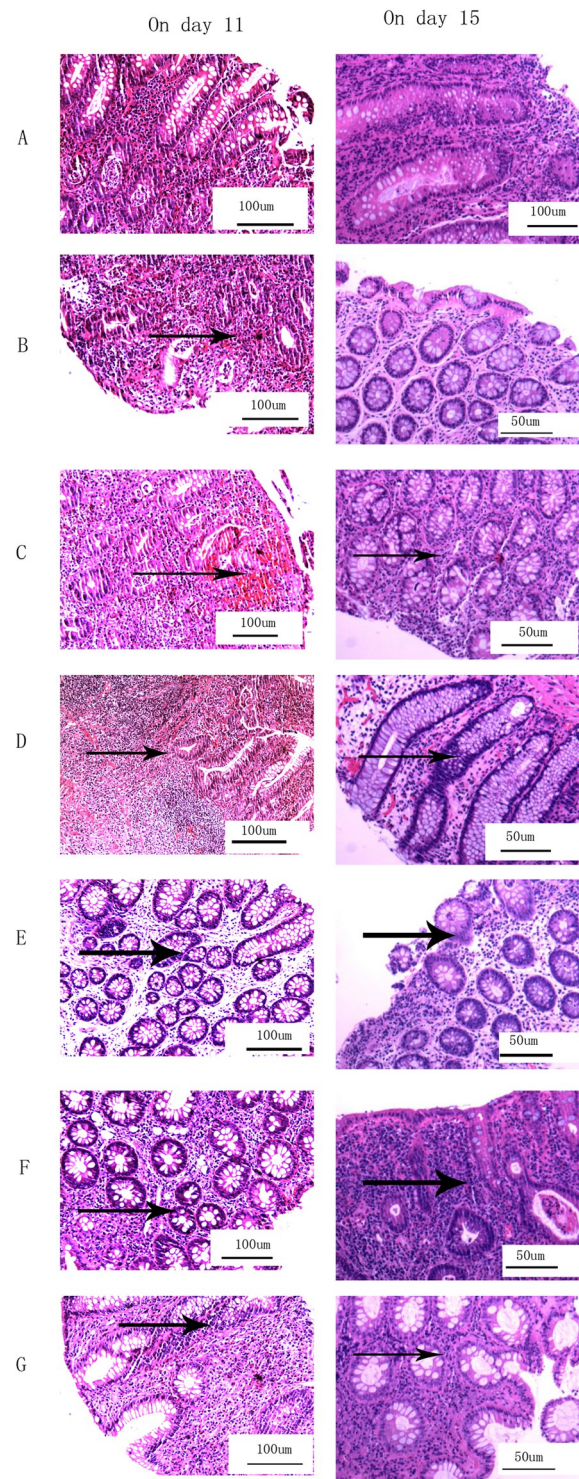


Fig 8. Pathological images of colonic hematoxylin-eosin staining. Images from groups (A) A, (B) B, (C) C, (D) D, (E) E, (F) F and (G) G. Left, rat colon tissue on day 11; right, rat colon tissue on day 15. In group A, no obvious neutrophil infiltration and mucosal edema were observed. In groups B-G, neutrophil infiltration was severe, and marked mucosal edema was notable; additionally, mucosal necrosis was observed, and focal ulcers were formed.

<https://doi.org/10.1371/journal.pone.0264194.g008>

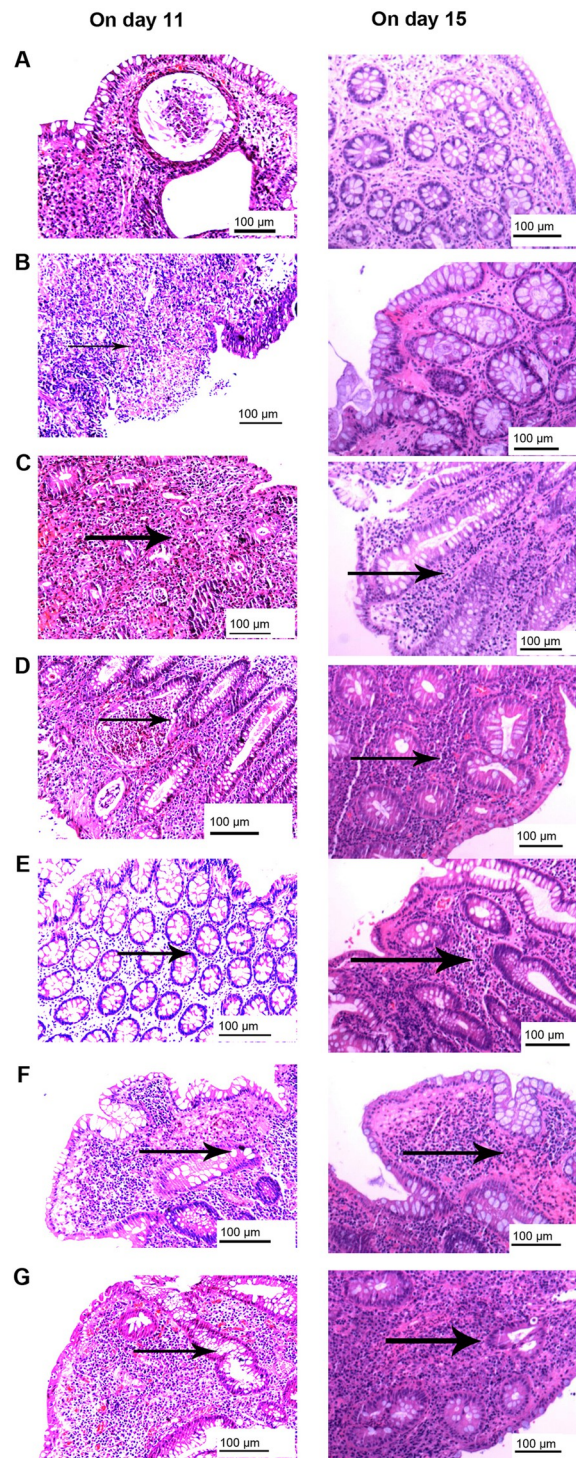


Fig 9. Pathological images of rectal tissue hematoxylin-eosin staining. Images from groups (A) A, (B) B, (C) C, (D) D, (E) E, (F) F and (G) G. Left, rat rectum tissue on day 11; right, rat rectum tissue on day 15. In group A, no obvious neutrophil infiltration and mucosal edema were observed. In groups B-G, neutrophil infiltration was severe, and marked mucosal edema was notable; additionally, mucosal necrosis was observed, and focal ulcers were formed.

<https://doi.org/10.1371/journal.pone.0264194.g009>

Conclusion

The present study indicated that it is feasible to establish an antibiotic-induced IBD model in SD rats, which may provide useful models for clinical IBD research.

Supporting information

S1 Table. Sequences of primers used for quantitative PCR.

(DOCX)

S2 Table. Comparison of basic status of rats across the study period (days 1,3,5,7 and 9).

(DOCX)

S3 Table. Comparison of total nine microbiota across days 1, 3, 5, 7, 9, 11 and 14 between the experimental groups.

(DOCX)

S4 Table. Comparison of inflammation factors between groups.

(DOCX)

S5 Table. Comparisons of inflammation scores in colon and rectum of animals.

(DOCX)

S1 Raw image. Fecal bacterial content and gut inflammation scores. (A) Comparison of bacterial amplification via quantitative PCR in groups A, C and F;(B) *Bacteroides*, *F. prausnitzii* and *D. invisus* agarose electrophoresis; (C) Comparison of colonic and rectal tissue inflammation scores on day 11 and day 15;(D) Comparison of colonic and rectal tissue inflammation scores of control group vs experiment groups respectively, *P<0.05, **P<0.01).

(PDF)

Acknowledgments

We thank Professor Licheng Dai, Professor Liqin Li, Professor Yingrong Chen, Professor Zhihong Ma (all Central Laboratory, Huzhou Central Hospital) for suggestions regarding the study. We also thank Dr Wei Fang (Department of Pathology, Huzhou Central Hospital) for analyzing and scoring the colonic and rectal tissue slices. Meanwhile we thank the research teams of Xi'an United Nations Quality Detection Technology Co., Ltd. Laboratory to perform the experiments.

Author Contributions

Conceptualization: Guojun Tong, Hai Qian, Jing Li, Xiongfeng Li.

Data curation: Guojun Tong, Dongli Li, Jing Chen.

Formal analysis: Guojun Tong, Hai Qian.

Funding acquisition: Guojun Tong, Hai Qian, Dongli Li, Jing Li, Xiongfeng Li.

Investigation: Guojun Tong.

Methodology: Hai Qian.

Software: Jing Li.

Validation: Jing Chen, Xiongfeng Li.

Writing – original draft: Guojun Tong.

Writing – review & editing: Guojun Tong, Dongli Li, Jing Chen.

References

1. Jacobs J. P., Goudarzi M., Singh N., Tong M., McHardy I. H., Ruegger P., et al. A Disease-Associated Microbial and Metabolomics State in Relatives of Pediatric Inflammatory Bowel Disease Patients[J]. *Cell Mol Gastroenterol Hepatol*, 2016, 2(6): 750–766. <https://doi.org/10.1016/j.jcmgh.2016.06.004> PMID: 28174747
2. Yang C, Merlin D. Naoparticle-Mediated Drug Delivery Systems For Treatment of IBD:Current perspectives.[J].*Int J Nanomedicine*.2019 Nov13; 14:8875–8889. <https://doi.org/10.2147/IJN.S210315> PMID: 32009785
3. Lin L, Zhang J. Role of intestinal microbiota and metabolites on gut homeostasis and human disease. [J].*BMC Immunol*.2017 Jan 6; 18(1):2.
4. Srikanth C. V. and Cherayil B. J. Intestinal innate immunity and the pathogenesis of Salmonella enteritis [J]. *Immunologic research*, 2007, 37(1): 61–78. <https://doi.org/10.1007/BF02686090> PMID: 17496347
5. Pelloquin J. M. and Nguyen D. D. The microbiota and inflammatory bowel disease: insights from animal models[J]. *Anaerobe*, 2013, 24: 102–106. <https://doi.org/10.1016/j.anaerobe.2013.04.006> PMID: 23603043
6. He C, Shi Y, Wu R, Sun M, Fang L, Wu W, et al. miR-301a promotes intestinal mucosal inflammation through induction of IL-17a and TNF- α in IBD.
7. Amoroso Chiara, Perillo Federica, Strati Francesco, Fantini Massimo, Caprioli Flavio, Facciotti Federica. The role of Gut Microbiota Biomodulators on Mucosal Immunity and Intestinal Inflammation.[J]. *Cells*.2020 May; 9(5):1234. <https://doi.org/10.3390/cells9051234> PMID: 32429359
8. Matowicka-Karna J. Makers of inflammation, activation of blood platelets and coagulation disorders in inflammatory bowel diseases.[J].*Postepy Hig Med Dosw(online)*.2016 Apr 13; 70:305–12.
9. Uzal F. A., McClane B. A., Cheung J. K., Theoret J., Garcia J. P., Moore, et al. Animal models to study the pathogenesis of human and animal Clostridium perfringens infections[J]. *Veterinary microbiology*, 2015, 179(1–2): 23–33. <https://doi.org/10.1016/j.vetmic.2015.02.013> PMID: 25770894
10. Jiminez J. A., Uwiera T. C., Douglas Inglis G. and Uwiera R. R. E. Animal models to study acute and chronic intestinal inflammation in mammals[J]. *Gut pathogens*, 2015, 7: 29–29. <https://doi.org/10.1186/s13099-015-0076-y> PMID: 26561503
11. Kuriyama Tomoko, Yamato Masayuki, Homma Jun, YusukeTobe, and Tokushige Katsutoshi. A novel rat model of inflammatory bowel disease developed using a device created with a 3D printer. *Regen Ther*. 2020 Jun; 14: 1–10. <https://doi.org/10.1016/j.reth.2019.12.005> PMID: 31970267
12. Naga K.R. Ghattamaneni, Sunil K. Panchal, Lindsay Brow. An improved rat model for chronic inflammatory bowel disease. *Pharmacological Reports Volume 71, Issue 1, February 2019, Pages 149–155.* <https://doi.org/10.1016/j.pharep.2018.10.006> PMID: 30550995
13. Catana CS, Magdas C, Tabaran FA, Cracium EC, Deak G, Magdas VA, et al. Comparison of two models of inflammatory bowel disease in rats. <https://doi.org/10.17219/acem/69134> PMID: 29616750
14. Jianmei Z.1, Mincong H.1, Yangling L.2, Bo Z.2, and Nengming L1. Comparison on the Model Rats with Colitis Induced by 2, 4, 6-three Nitrobenzene Sulfonic Acid and Dex-tran Sulfate Sodium[J]. *China pharmacy*, 2017, 28(10): 1353–1356.
15. HU Tingting C. H. Establishment of acute radiation proctitis model in rats[J]. *Journal of Clinical Oncology*, 2019, 24(7): 584–587.
16. CHEN Suao, JIN Shizhu. Murine model of dextran sodium sulfate-induced ulcerative colitis.[J].*Chin J Comp Med*,2020, 30(4):142–146. <https://doi.org/10.1093/ppar/praa023> PMID: 33214754
17. Lanfeng Zhang, Xixia Zhang, Yunfang Qiu, Jianhua Jin, Shunxin Zhu, Jianting Wu, et al. Establishment and evaluation of the rat retention enema treatments model for acute radiation proctitis.[J] *Journal of advanced nursing education*,2011, 26(23):2117–2119.
18. Maria Jose Saez-Lara Carolina Gomez-Llorente, Julio Plaza-Diaz Angel Gil. The Role of Probiotic Lactic Acid Bacteria and Bifidobacteria in the Prevention and Treatment of Inflammatory Bowel Disease and Other Related Diseases: A Systematic Review of Randomized Human Clinical Trials. *Biomed Res Int*. 2015; 2015: 505878. Published online 2015 Feb 22. <https://doi.org/10.1155/2015/505878> PMID: 25793197
19. Zhou Bolun, Yuan Yutong, Zhang Shanshan, Guo Can, Li Xiaoling, Li Guiyuan, et al. Intestinal Flora and Disease Mutually Shape the Regional Immune System in the Intestinal Tract. *Front Immunol*. 2020; 11: 575. Published online 2020 Apr 3. <https://doi.org/10.3389/fimmu.2020.00575> PMID: 32318067

20. HongleWu YueMa, XianPeng WeiQiu, LixinKong BiaoRen, et al. Antibiotic-induced dysbiosis of the rat oral and gut microbiota and resistance to Salmonella. *Archives of Oral Biology*. Volume 114, June 2020, 104730. <https://doi.org/10.1016/j.archoralbio.2020.104730> PMID: 32371145
21. Alexandra C Vaughn, Erin M Cooper, Patricia M DiLorenzo, Levi J O'Loughlin, Michael E Konkel, James H Peters, et al. Energy-dense diet triggers changes in gut microbiota, reorganization of gut-brain vagal communication and increases body fat accumulation. *Acta Neurobiol Exp (Wars)*. 2017; 77(1):18–30. <https://doi.org/10.21307/ane-2017-033> PMID: 28379213
22. CASSETTE—clindamycin adjunctive therapy for severe Staphylococcus aureus treatment evaluation: study protocol for a randomised controlled trial. *Trials*. 2019; 20: 353. Published online 2019 Jun 13. <https://doi.org/10.1186/s13063-019-3452-y> PMID: 31196132
23. Whittemore Jacqueline C., Stokes Jennifer E., Price Joshua M., Suchodolski Jan S. Effects of a synbiotic on the fecal microbiome and metabolomic profiles of healthy research cats administered clindamycin: a randomized, controlled trial. *Gut Microbes*. 2019; 10(4): 521–539. Published online 2019 Feb 1. <https://doi.org/10.1080/19490976.2018.1560754> PMID: 30709324
24. Ghai Ishan, Bajaj Harsha, Jayesh Arun Bafna Hussein Ali El Damrany Hussein, Winterhalter Mathias, Wagner Richard. Ampicillin permeation across OmpF, the major outer-membrane channel in *Escherichia coli*. <https://doi.org/10.1074/jbc.RA117.000705> PMID: 29540483
25. Ahmad Amais, Zachariassen Camilla, Lasse Engbo Christiansen Kaare Græsbøll, Toft Nils, Matthews Louise, et al. Modeling the growth dynamics of multiple *Escherichia coli* strains in the pig intestine following intramuscular ampicillin treatment. *BMC Microbiol*. 2016; 16(1): 205. Published online 2016 Sep 6. <https://doi.org/10.1186/s12866-016-0823-3> PMID: 27599570
26. Singh Atul K., Drolia Rishi, Bai Xingjian, Bhunia Arun K. Streptomycin Induced Stress Response in *Salmonella enterica* Serovar Typhimurium Shows Distinct Colony Scatter Signature. *PLoS One*. 2015; 10(8): e0135035. Published online 2015 Aug 7. <https://doi.org/10.1371/journal.pone.0135035> PMID: 26252374
27. Pindling Sydney, Azulai Daniella, Zheng Brandon, Dahan Dylan, Gabriel G Perron. Dysbiosis and early mortality in zebrafish larvae exposed to subclinical concentrations of streptomycin. *FEMS Microbiol Lett*. 2018 Sep; 365(18): fny188. Published online 2018 Jul 31. <https://doi.org/10.1093/femsle/fny188> PMID: 30085054
28. National Research Council (US) Institute for Laboratory Animal Research. *Guide for the Care and Use of Laboratory Animals*. Washington (DC): National Academies Press (US); 1996.
29. Sangfelt P, Carlson M, Thörn M, Löf L, Raab Y. Neutrophil and eosinophil granule proteins as markers of response to local prednisolone treatment in distal ulcerative colitis and proctitis. *Am J Gastroenterol*. 2001 Apr; 96(4):1085–90. <https://doi.org/10.1111/j.1572-0241.2001.03743.x> PMID: 11316151
30. Kanneganti M., Mino-Kenudson M. and Mizoguchi E. Animal models of colitis-associated carcinogenesis [J]. *J Biomed Biotechnol*, 2011, 2011: 342637. <https://doi.org/10.1155/2011/342637> PMID: 21274454
31. De Zuani M, Dal Secco C, Frossi B. Mast cells at the crossroads of microbiota and IBD. [J]. *Eur J Immunol*. Dec 2018; 48(12):1929–1973. <https://doi.org/10.1002/eji.201847504> PMID: 30411335
32. Green N, Miller T, Sukind D. A Review of Dietary for IBD and a vision for the Future. [J]. *Nutrients*. Apr 26, 2019; 11(5).
33. Karen M. O'Connor, Eric F. Lucking, Anna V. Golubeva, Conall R. Strain, Fiona Fouhy, María C. Cenit, et al. Manipulation of gut microbiota blunts the ventilatory response to hypercapnia in adult rats. *EBio-Medicine*. 2019 Jun; 44: 618–638. Published online 2019 Mar 18. <https://doi.org/10.1016/j.ebiom.2019.03.029> PMID: 30898652
34. Tong S. Y. C., Davis J. S., Eichenberger E., Holland T. L. and Fowler V. G. Jr. *Staphylococcus aureus* infections: epidemiology, pathophysiology, clinical manifestations, and management [J]. *Clinical microbiology reviews*, 2015, 28(3): 603–661. <https://doi.org/10.1128/CMR.00134-14> PMID: 26016486
35. Balasubramanian D., Harper L., Shopsin B. and Torres V. J. *Staphylococcus aureus* pathogenesis in diverse host environments [J]. *Pathogens and disease*, 2017, 75(1): ftx005. <https://doi.org/10.1093/femspd/ftx005> PMID: 28104617
36. Kim B. J., Park T., Moon H. C., Park S. Y., Hong D., Ko E. H., et al. Cytoprotective alginate/polydopamine core/shell microcapsules in microbial encapsulation [J]. *Angew Chem Int Ed Engl*, 2014, 53(52): 14443–14446. <https://doi.org/10.1002/anie.201408454> PMID: 25354197
37. Dzialo M. C., Park R., Steensels J., Lievens B. and Verstrepen K. J. Physiology, ecology and industrial applications of aroma formation in yeast [J]. *FEMS Microbiol Rev*, 2017, 41(Supp_1): S95–s128. <https://doi.org/10.1093/femsre/fux031> PMID: 28830094
38. Rakoff-Nahoum S, Foster KR, Comstock LE. The evolution of cooperation in the gut microbiota. [J]. *Nature*. 2016 May 12; 533(7602):255–9. <https://doi.org/10.1038/nature17626> PMID: 27111508

39. Yu SY, Kim JS, Oh BS, Park SH, Kang SW, Park JE, et al. *Bacteroides faecalis* sp.nov., isolated from human faeces.[J]. *Int J Syst Evol Microbiol*. 2019 Dec; 69(12):3824–3829. <https://doi.org/10.1099/ijsem.0.003690> PMID: 31511127
40. Paredes C. J., Alsaker K. V. and Papoutsakis E. T. A comparative genomic view of clostridial sporulation and physiology[J]. *Nat Rev Microbiol*, 2005, 3(12): 969–978. <https://doi.org/10.1038/nrmicro1288> PMID: 16261177
41. Gajdacs M., Spengler G. and Urban E. Identification and Antimicrobial Susceptibility Testing of Anaerobic Bacteria: Rubik's Cube of Clinical Microbiology?[J]. *Antibiotics* (Basel), 2017, 6(4).
42. Croxen M. A., Law R. J., Scholz R., Keeney K. M., Wlodarska M. and Finlay B. B. Recent advances in understanding enteric pathogenic *Escherichia coli*[J]. *Clin Microbiol Rev*, 2013, 26(4): 822–880. <https://doi.org/10.1128/CMR.00022-13> PMID: 24092857
43. Golinska E., Tomusiak A., Gosiewski T., Wiecek G., Machul A., Mikolajczyk D., et al. Virulence factors of *Enterococcus* strains isolated from patients with inflammatory bowel disease[J]. *World J Gastroenterol*, 2013, 19(23): 3562–3572. <https://doi.org/10.3748/wjg.v19.i23.3562> PMID: 23801857
44. Inglin R. C., Meile L. and Stevens M. J. A. Clustering of Pan- and Core-genome of *Lactobacillus* provides Novel Evolutionary Insights for Differentiation[J]. *BMC Genomics*, 2018, 19(1): 284. <https://doi.org/10.1186/s12864-018-4601-5> PMID: 29690879
45. Helena Mendes-Soares Haruo Suzuki, Roxana J Hickey, Larry J Fomey. Comparative Functional Genomics of *Lactobacillus* spp. Reveals Possible Mechanisms for Specialization of Vaginal *Lactobacilli* to Their Environment..[J] *J Bacteriol*. 2014 Apr, 196(7):1458–1470. <https://doi.org/10.1128/JB.01439-13> PMID: 24488312
46. Liu Xi, Zheng Hua, Lu Rigang, Huang Huimin, Zhu Hongjia, Yin Chunli, et al. Intervening Effects of Total Alkaloids of *Corydalis saxicola* Bunting on Rats With Antibiotic-Induced Gut Microbiota Dysbiosis Based on 16S rRNA Gene Sequencing and Untargeted Metabolomics Analyses. *Front Microbiol*. 2019; 10: 1151. Published online 2019 May 31. <https://doi.org/10.3389/fmicb.2019.01151> PMID: 31214133
47. Yu Meng, Jia Hong-Mei, Zhou Chao, Yang Yong, Sun Li-Li, Zou Zhong-Mei. Urinary and Fecal Metabonomics Study of the Protective Effect of Chaihu-Shu-Gan-San on Antibiotic-Induced Gut Microbiota Dysbiosis in Rats. *Sci Rep*. 2017; 7: 46551. Published online 2017 Apr 20. <https://doi.org/10.1038/srep46551> PMID: 28425490
48. Caputi Valentina, Marsilio Ilaria, Filpa Viviana, Cerantola Silvia, Orso Genny, Bistoletti Michela, et al. Antibiotic-induced dysbiosis of the microbiota impairs gut neuromuscular function in juvenile mice. *Br J Pharmacol*. 2017; 174(20): 3623–3639. Published online 2017 Aug 30. <https://doi.org/10.1111/bph.13965> PMID: 28755521
49. Farzi Aitak, Esther E. Fröhlich, Peter Holzer. Gut Microbiota and the Neuroendocrine System. *Neurotherapeutics*. 2018 Jan; 15(1): 5–22. Published online 2018 Jan 27. <https://doi.org/10.1007/s13311-017-0600-5> PMID: 29380303
50. Esther E. Fröhlich, Aitak Farzi, Raphaela Mayerhofer, Florian Reichmann, Angela Jačan, Bernhard Wagner, et al. Cognitive Impairment by Antibiotic-Induced Gut Dysbiosis: Analysis of Gut Microbiota-Brain Communication. *Brain Behav Immun*. Author manuscript; available in PMC 2016 Sep 7. Published in final edited form as: *Brain Behav Immun*. 2016 Aug; 56: 140–155. Published online 2016 Feb 23. <https://doi.org/10.1016/j.bbi.2016.02.020> PMID: 26923630
51. Claire Buchta Rosean Raegan R. Bostic, Ferey Joshua C. M., Feng Tzu-Yu, Azar Francesca N., Tung Kenneth S., et al. Rutkowski. Pre-existing commensal dysbiosis is a host-intrinsic regulator of tissue inflammation and tumor cell dissemination in hormone receptor-positive breast cancer. *Cancer Res*. Author manuscript; available in PMC 2020 Jul 15. Published in final edited form as: *Cancer Res*. 2019 Jul 15; 79(14): 3662–3675. Published online 2019 May 7. <https://doi.org/10.1158/0008-5472.CAN-18-3464> PMID: 31064848
52. Jenkins Samir V., Robeson Michael S. II, Griffin Robert J., Quick Charles M., Siegel Eric R., Cannon Martin J., et al. Dings. Gastrointestinal tract dysbiosis enhances distal tumor progression through suppression of leukocyte trafficking. *Cancer Res*. Author manuscript; available in PMC 2020 Jun 1. Published in final edited form as: *Cancer Res*. 2019 Dec 1; 79(23): 5999–6009. Published online 2019; Ct 7. <https://doi.org/10.1158/0008-5472.CAN-18-4108> PMID: 31591154
53. Miyoshi Jun, Bobe Alexandria M., Miyoshi Sawako, Huang Yong, Hubert Nathaniel, Delmont Tom O., et al. Peripartum exposure to antibiotics promotes persistent gut dysbiosis, immune imbalance, and inflammatory bowel disease in genetically prone offspring. *Cell Rep*. Author manuscript; available in PMC 2017 Nov 2. Published in final edited form as: *Cell Rep*. 2017 Jul 11; 20(2): 491–504. <https://doi.org/10.1016/j.celrep.2017.06.060> PMID: 28700948
54. Hagihara Mao, Kuroki Yasutoshi, Ariyoshi Tadashi, Higashi Seiya, Fukuda Kazuo, Yamashita Rieko, et al. *Clostridium butyricum* Modulates the Microbiome to Protect Intestinal Barrier Function in Mice with Antibiotic-Induced Dysbiosis. *iScience*. 2020 Jan 24; 23(1): 100772. Published online 2019 Dec 13. <https://doi.org/10.1016/j.isci.2019.100772> PMID: 31954979

55. Kanwal Sadia, Thomson Patrick Joseph Lawrence Owusu, Xiaomeng Ren, Meiqi Li, Yi Xin. A Polysaccharide Isolated from *Dictyophora indusiata* Promotes Recovery from Antibiotic-Driven Intestinal Dysbiosis and Improves Gut Epithelial Barrier Function in a Mouse Model. *Nutrients*. 2018 Aug; 10(8): 1003. Published online 2018 Jul 31. <https://doi.org/10.3390/nu10081003> PMID: 30065236
56. Arivarasu N, Anbazhagan, Shubha Priyamvada, Waddah A Alrefai, Dudeja. Pathophysiology of IBD associated diarrhea. *J Tissue Barriers*. 2018; 6(2).
57. Zhou Yingting, Zhi Fachao. Lower Level of *Bacteroides* in the Gut Microbiota Is Associated with Inflammatory Bowel Disease: A Meta-Analysis. *Biomed Res Int*. 2016; 2016: 5828959. Published online 2016 Nov 24. <https://doi.org/10.1155/2016/5828959> PMID: 27999802
58. Mireia Lopez-Siles N ria Enrich-Cap , Aldeguer Xavier, Miriam Sabat-Mir Sylvia H. Duncan, Jes s Garcia-Gil L., et al. Alterations in the Abundance and Co-occurrence of *Akkermansia muciniphila* and *Faecalibacterium prausnitzii* in the Colonic Mucosa of Inflammatory Bowel Disease Subjects. *Front Cell Infect Microbiol*. 2018; 8: 281. Published online 2018 Sep 7. <https://doi.org/10.3389/fcimb.2018.00281> PMID: 30245977
59. Khan Israr, Ullah Naeem, Zha Lajia, Bai Yanrui, Khan Ashiq, Zhao Tang, et al. Alteration of Gut Microbiota in Inflammatory Bowel Disease (IBD): Cause or Consequence? IBD Treatment Targeting the Gut Microbiome. *Pathogens*. 2019 Sep; 8(3): 126. Published online 2019 Aug 13. <https://doi.org/10.3390/pathogens8030126> PMID: 31412603
60. Zafar H. and Saier M. H. Jr. Comparative genomics of transport proteins in seven *Bacteroides* species [J]. *PLoS one*, 2018, 13(12): e0208151–e0208151. <https://doi.org/10.1371/journal.pone.0208151> PMID: 30517169
61. Vineis J. H., Ringus D. L., Morrison H. G., Delmont T. O., Dalal S., Raffals L. H., et al. Patient-Specific *Bacteroides* Genome Variants in Pouchitis [J]. *mBio*, 2016, 7(6): e01713–01716. <https://doi.org/10.1128/mBio.01713-16> PMID: 27935837
62. Feng S. and McLellan S. L. Highly Specific Sewage-Derived *Bacteroides* Quantitative PCR Assays Target Sewage-Polluted Waters [J]. *Applied and environmental microbiology*, 2019, 85(6): e02696–02618. <https://doi.org/10.1128/AEM.02696-18> PMID: 30635376
63. Lopez-Siles M., Duncan S. H., Garcia-Gil L. J. and Martinez-Medina M. *Faecalibacterium prausnitzii*: from microbiology to diagnostics and prognostics [J]. *The ISME journal*, 2017, 11(4): 841–852. <https://doi.org/10.1038/ismej.2016.176> PMID: 28045459
64. Munukka E., Rintala A., Toivonen R., Nylund M., Yang B., Takanen A., et al. *Faecalibacterium prausnitzii* treatment improves hepatic health and reduces adipose tissue inflammation in high-fat fed mice [J]. *The ISME journal*, 2017, 11(7): 1667–1679. <https://doi.org/10.1038/ismej.2017.24> PMID: 28375212
65. Schirmer M., Franzosa E. A., Lloyd-Price J., McIver L. J., Schwager R., Poon T. W., et al. Dynamics of metatranscription in the inflammatory bowel disease gut microbiome [J]. *Nature microbiology*, 2018, 3(3): 337–346. <https://doi.org/10.1038/s41564-017-0089-z> PMID: 29311644
66. Leonard M., Ryan M. P., Watson A. J., Schramek H. and Healy E. Role of MAP kinase pathways in mediating IL-6 production in human primary mesangial and proximal tubular cells [J]. *Kidney Int*, 1999, 56(4): 1366–1377. <https://doi.org/10.1046/j.1523-1755.1999.00664.x> PMID: 10504489
67. Amrani Y., Ammit A. J. and Panettieri R. A. Jr. Tumor necrosis factor receptor (TNFR) 1, but not TNFR2, mediates tumor necrosis factor- α -induced interleukin-6 and RANTES in human airway smooth muscle cells: role of p38 and p42/44 mitogen-activated protein kinases [J]. *Mol Pharmacol*, 2001, 60(4): 646–655. PMID: 11562425
68. Coelho-Santos V., Gonalves J., Fontes-Ribeiro C. and Silva A. P. Prevention of methamphetamine-induced microglial cell death by TNF- α and IL-6 through activation of the JAK-STAT pathway [J]. *Journal of neuroinflammation*, 2012, 9: 103–103. <https://doi.org/10.1186/1742-2094-9-103> PMID: 22642790
69. Kanamori Y., Murakami M., Sugiyama M., Hashimoto O., Matsui T. and Funaba M. Interleukin-1 β (IL-1 β) transcriptionally activates hepcidin by inducing CCAAT enhancer-binding protein δ (C/EBP δ) expression in hepatocytes [J]. *The Journal of biological chemistry*, 2017, 292(24): 10275–10287. <https://doi.org/10.1074/jbc.M116.770974> PMID: 28438835
70. Sudhakar M., Silambanan S., Chandran A. S., Prabhakaran A. A. and Ramakrishnan R. C-Reactive Protein (CRP) and Leptin Receptor in Obesity: Binding of Monomeric CRP to Leptin Receptor [J]. *Frontiers in immunology*, 2018, 9: 1167–1167. <https://doi.org/10.3389/fimmu.2018.01167> PMID: 29910808
71. Lee P. T., Bird S., Zou J. and Martin S. A. M. Phylogeny and expression analysis of C-reactive protein (CRP) and serum amyloid-P (SAP) like genes reveal two distinct groups in fish [J]. *Fish & shellfish immunology*, 2017, 65: 42–51.
72. S ndberg E., Sinha A. K., Gerdes K. and Semsey S. CRP Interacts Specifically With Sxy to Activate Transcription in *Escherichia coli* [J]. *Frontiers in microbiology*, 2019, 10: 2053–2053. <https://doi.org/10.3389/fmicb.2019.02053> PMID: 31543875

73. Roulis M., Bongers G., Armaka M., Salviano T., He Z., Singh A., et al. Host and microbiota interactions are critical for development of murine Crohn's-like ileitis[J]. *Mucosal immunology*, 2016, 9(3): 787–797. <https://doi.org/10.1038/mi.2015.102> PMID: 26487367
74. Bastaki S. M. A., Al Ahmed M. M., Al Zaabi A., Amir N. and Adeghate E. Effect of turmeric on colon histology, body weight, ulcer, IL-23, MPO and glutathione in acetic-acid-induced inflammatory bowel disease in rats[J]. *BMC complementary and alternative medicine*, 2016, 16: 72–72. <https://doi.org/10.1186/s12906-016-1057-5> PMID: 26907175
75. Almohazey D., Lo Y.-H., Vossler C. V., Simmons A. J., Hsieh J. J., Bucar E. B., et al. The ErbB3 receptor tyrosine kinase negatively regulates Paneth cells by PI3K-dependent suppression of Atoh1[J]. *Cell death and differentiation*, 2017, 24(5): 855–865. <https://doi.org/10.1038/cdd.2017.27> PMID: 28304405
76. Sokol H, Lay C, Seksik P, Tannock GW. Analysis of bacterial bowel communities of IBD patients: what has it revealed? *Inflammatory Bowel Diseases*. 2008; 14(6):858–67. <https://doi.org/10.1002/ibd.20392> PMID: 18275077
77. Czaja Krzysztof, Gaway Brent (2017) Broad-Spectrum Antibiotic Abuse and its Connection to Obesity. *J Nutrition Health Food Sci* 5(4):1–21. <http://dx.doi.org/10.15226/jnhfs.2017.001102>.